Table of Contents

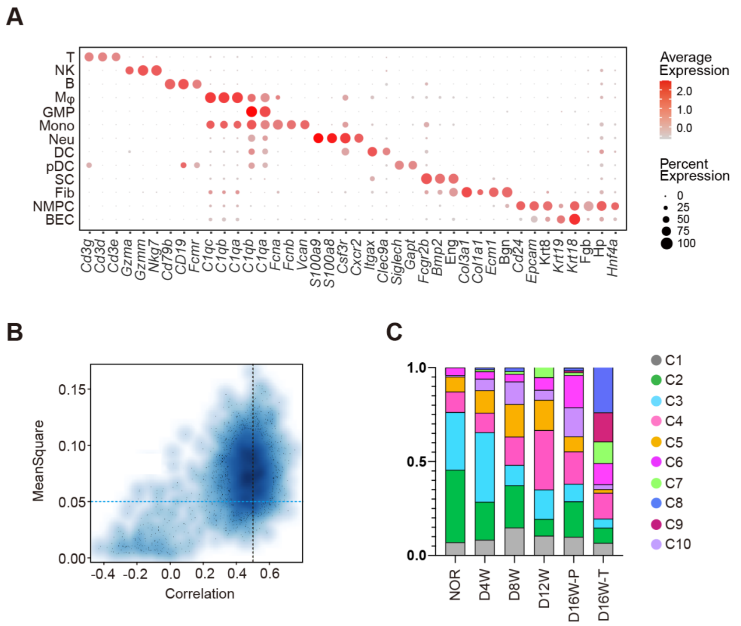

Appendix Figure S1. Identification of non-malignant and malignant cells from DEN-treated rats

A. Dot plots showing average expression of known markers in indicated cell types. Cells were annotated as T cells, B cells, natural killer (NK) cells, granulocytic/monocytic-restricted progenitors (GMP), monocytes (Mono), macrophages (Mφ), neutrophils (Neu), dendritic cells (DC), plasmacytoid dendritic cells (pDC), fibroblasts (Fib), non-malignant parenchymal cells (NMPC), bile duct epithelial cells (BEC) and stromal cells (SC) by known lineage-specific marker genes. **B.** Chromosomal copy-number variations (CNVs) were inferred from transcriptomes of the cells in rats, with SNV signal > 0.05 and correlation with tumor cells > 0.5. **C.** Stacked bar plots showing the proportions of different clusters in the 6 samples.

Related to **Figure 1**.

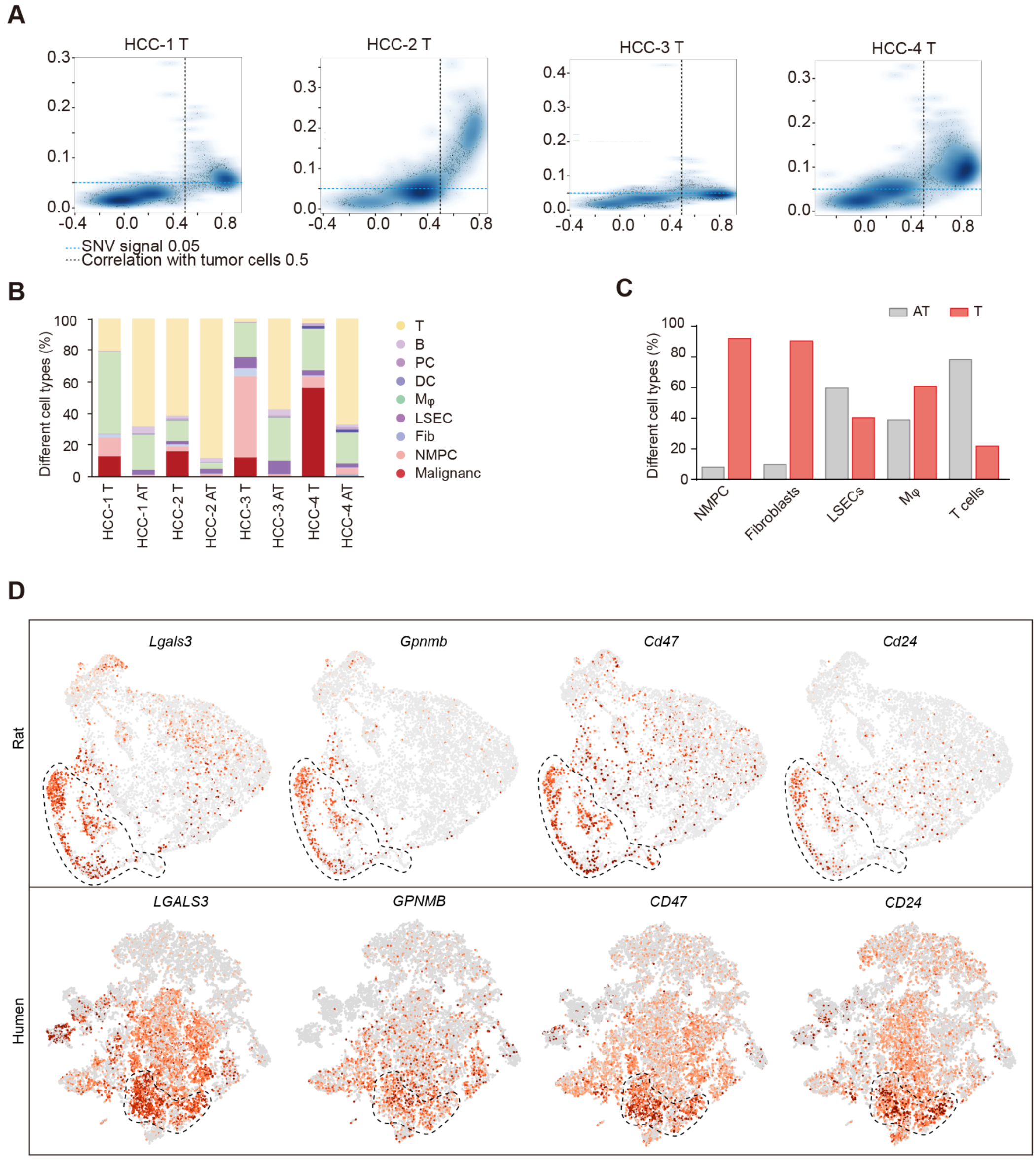

Appendix Figure S2. Identification of malignant cells and composition of each cell type in HCC patients

A. The definition of malignant cells by inferring CNV, with SNV signal > 0.05 and correlation with tumor cells > 0.5. **B.** Stacked bar plots showing the cellular composition of the 8 samples. **C.** Stacked bar plots showing the proportions of different cell types in tumors (T) and adjacent liver tissues (AT). **D.** The level of *LGALS3*, *GPNMB*, *CD47* and *CD24* in rats and patients.

Related to **Figure 2.**

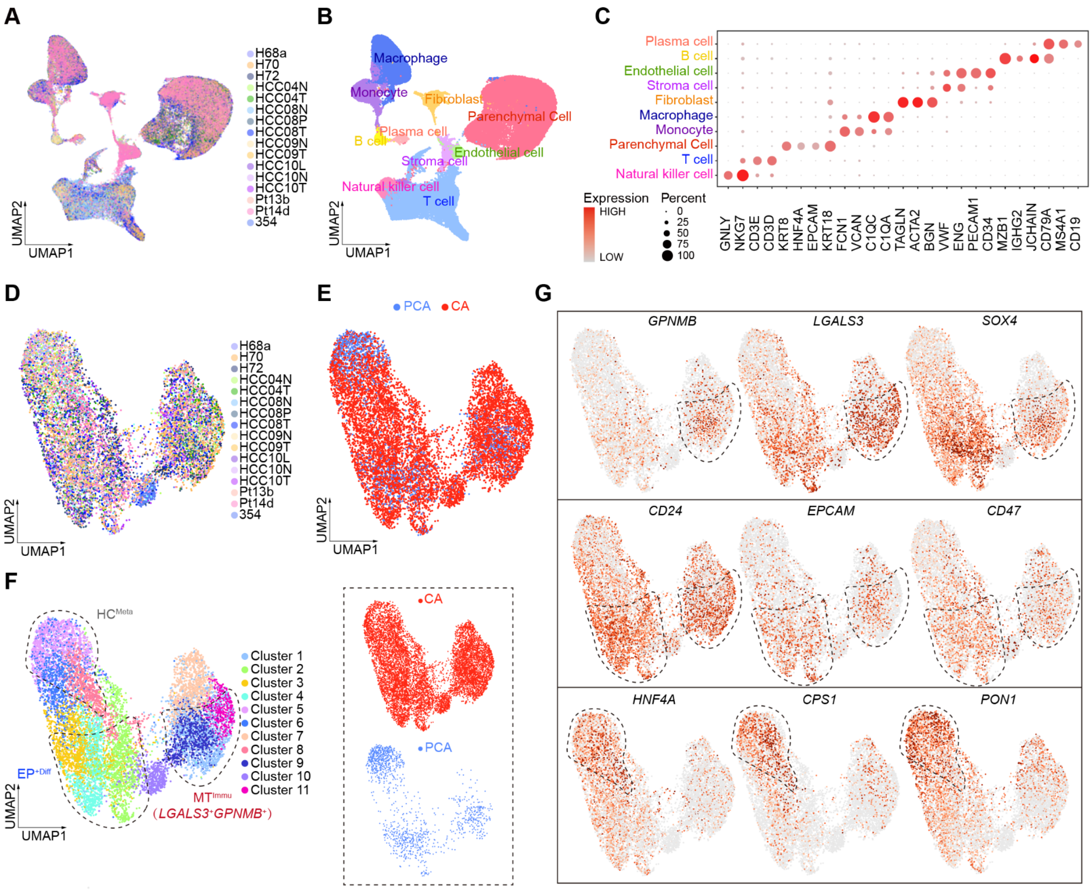

Appendix Figure S3. **Single cell RNA analyses of published data from HCC patients**

A. Tumor (T), adjacent liver tissue (N) and lymph gland metastasis (L) collection before processing for scRNA-seq by 10× Genomics. UMAP plot of all the single cells from 10 HCC patients (indicated by colors). **B.** UMAP plot showing classification and identification of all single cells. Cells were annotated as T cell, natural killer cell, B cell, plasma cell, endothelial cell, monocyte, macrophage, neutrophil, fibroblast, stromal cell, and parenchymal cells based lineage-specific marker genes (from A). **C.** Dot plots showing the average expression of selected markers in the indicated cell types. **D**. The parenchymal cells from 16 samples were shown by color-coded UMAP plot. **E**. UMAP colored by sample types. (N: blue; T: red). **F**. The parenchymal cells were further identified 11 distinct clusters (clusters 1-11), shown by color-coded UMAP plot. **G**. The level of genes in parenchymal cells of 10 HCC patients.

Related to **Figure 2.**

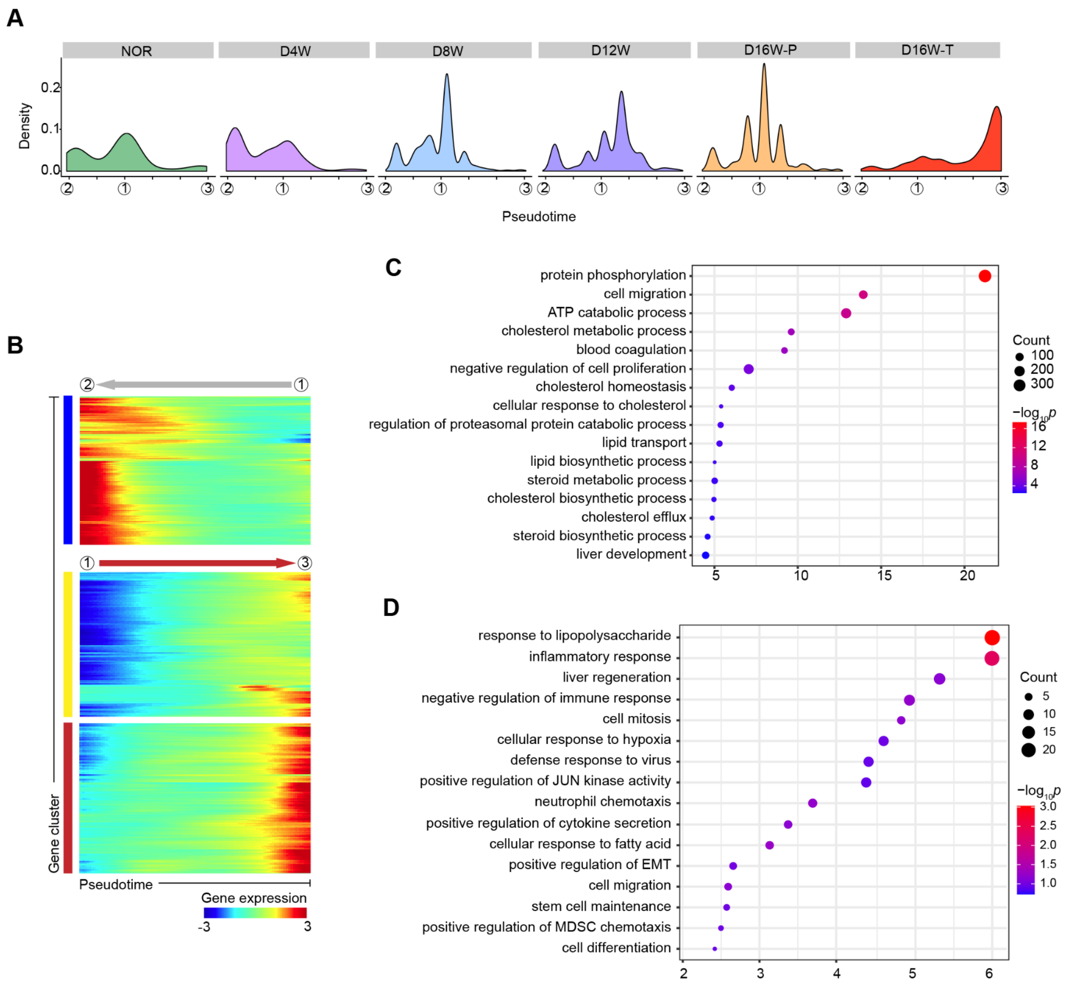

Appendix Figure S4. Molecular signatures in the trajectory of EP^{+Diff} transformed into HC^{Meta} or MT^{Immu}

A. Pseudotime of the composition of each time-point sample of rats. **B.** Heatmap showing the upregulated genes in branch ② and ③ as compared to branch ①. **C.** The Gene Ontology (GO) analysis of upregulated genes of branches ② in B. **D.** The Gene Ontology (GO) analysis of upregulated genes of branches ③ in B.

Related to **Figure 3.**

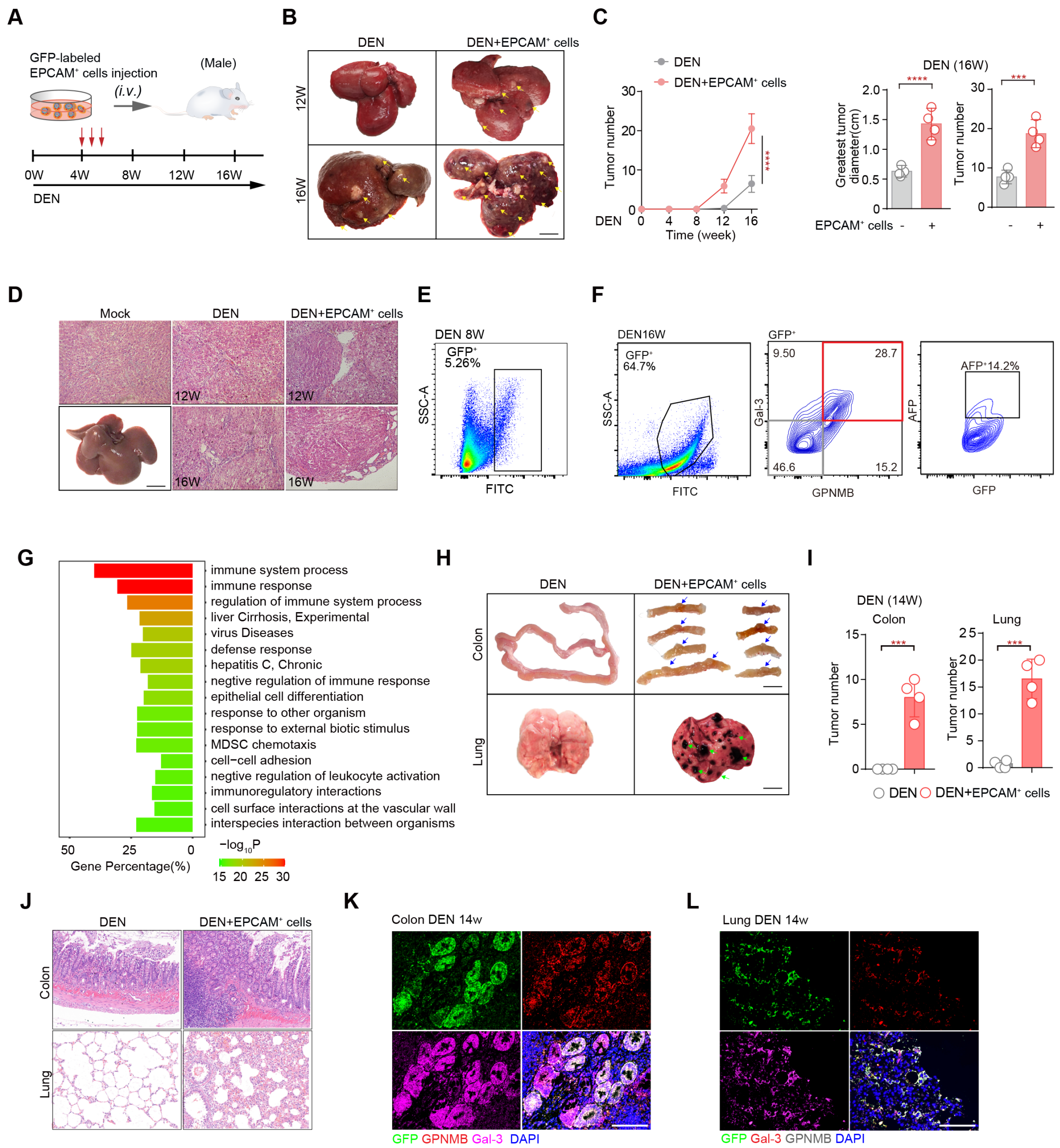

Appendix Figure S5. Characterization of the exogenous rat HCC model.

A. Injection of 1×10^8 GFP-labeled EPCAM$^+$ cells via tail vein into DEN-treated male rats (red arrows). **B.** Representative liver morphology of DEN-treated together with or without injection of GFP-labeled EPCAM$^+$ cells at 12 and 16 weeks. Yellow arrows indicated the tumor nodules in the liver. **C.** Tumor incidences of DEN-treated rats with or without GFP-labeled EPCAM$^+$ cells injection at 4, 8, 12 and 16 weeks (Left). The number and the greatest diameter of tumor nodules per liver were quantified at 16 weeks (Right). **D.** Representative liver morphology and hematoxylin-eosin (HE) staining of samples shown in B at 12 and 16 weeks. **E**. Flow cytometry analysis of GFP-labeled cells derived from GFP-labeled EPCAM$^+$ cells injected in DEN-treated rats at 2 weeks after injection. **F**. Flow cytometry analysis of GPNMB$^+$Gal-3$^+$, AFP$^+$ cells derived from GFP-labeled EPCAM$^+$ cells in DEN-treated rats at 16 weeks. **G.** The Gene Ontology (GO) analysis of upregulated genes in the GPNMB$^+$Gal-3$^+$ group. **H.** Representative colon and lung morphology of in rats exposed to DEN with or without GFP-labeled EPCAM$^+$ cells injection. **I.** The number of tumor nodules per colon and lung of (H). **J.** Representative colon and lung HE staining of (H). **K, L.** Staining of GFP, GPNMB, Gal-3 and DAPI in metastatic colon and lung tumors of (H), respectively. Bar, 100μm. At least two independent experiments were performed for all data. For curve figures and bar figures, data are presented as means ± SD. Unpaired Student's t-tests were used for comparing two variables. One-way ANOVA was used for multiple variables comparison. ***, $P < 0.001$; ****, $P < 0.0001$; n.s., no significance in comparison with the control group.

Related to **Figure 4.**

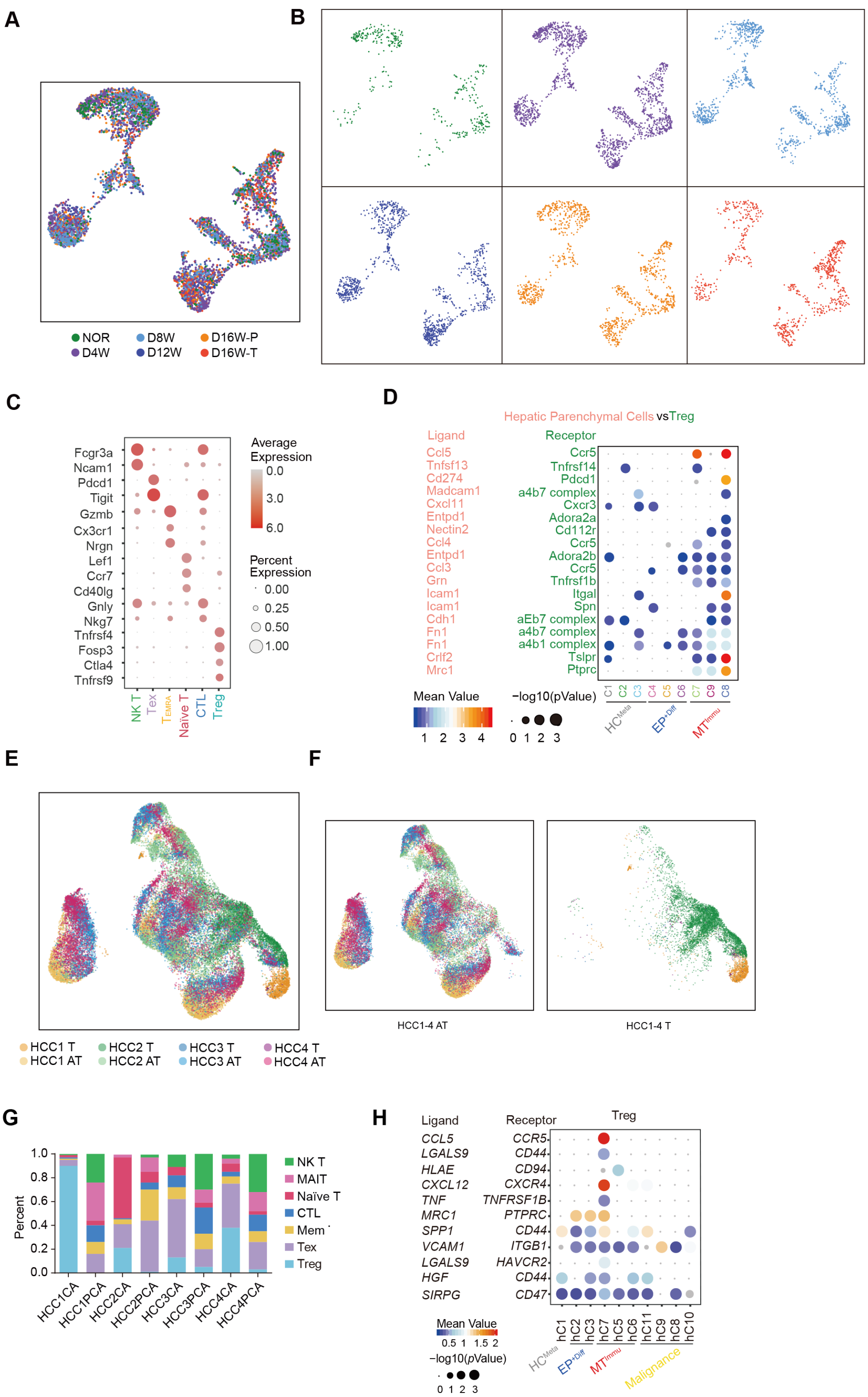

Appendix Figure S6. The distribution of T cells in HCC samples from rats and patients

A, B. UMAP plots of all the single cells of T cells from 6 samples of rats (indicated by colors). **C.** Dot plot showing the expression of canonical marker genes for annotating the

T cell subtypes. **D.** Bubble chart showing the expression of ligand-receptor pairs highly expressed between $HC^{Meta}/EP^{+Diff}/MT^{Immu}$ and regulatory T cells (Treg) in rats. **E.** UMAP plot of all the single cells of T cells from 4 HCC patients (indicated by colors). **F.** UMAP plot of the T cells from tumors (T) and adjacent liver tissues (AT) of 4 HCC patients. **G.** Stacked bar plots showing the frequency of T cell subtypes in HCC patients. **H.** Dot plot of L-R interactions between $HC^{Meta}/EP^{+Diff}/MT^{Immu}$/ malignance and Treg.

Related to **Figure 5.**

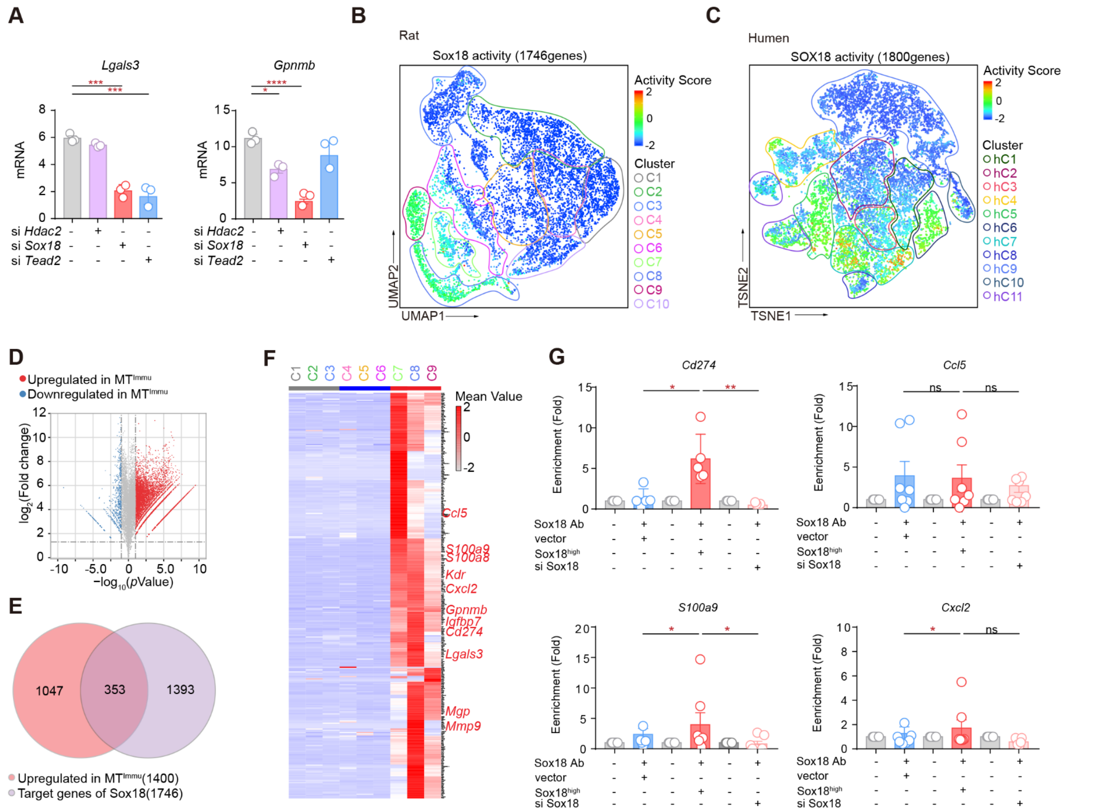

Appendix Figure S7. SOX18 Is associated with immunosuppression of GPNMB^{+}Gal-3^{+}MT^{Immu}

A. The mRNA levels of *Lgals3* and *Gpnmb* in *wild-type* (*WT*) and *Sox18-, Tead2-,* or *Hdac2*-depleted EPCAM^{+} cells. **B.** The specificity and activity scores of Sox18 in HC^{Meta}, EP^{+Diff} and MT^{Immu} of rats. **C.** The specificity and activity scores of SOX18 in HC^{Meta}, EP^{+Diff}, MT^{Immu} and malignance of HCC patients. **D.** Volcano plots exhibiting upregulated and downregulated genes in MT^{Immu}. **E.** Overlap of upregulated genes in MT^{Immu} and target genes of Sox18. **F.** The level of 353 genes of E in HC^{Meta}, EP^{+Diff} and MT^{Immu} (clusters C1-9). **G.** ChIP experiment of *Cd274*, *Ccl5*, *S100a9* and *Cxcl2* performed with Sox18 antibody in *WT, Sox18*-overexpressing and *Sox18*-knockdown EPCAM^{+} cells. At least two independent experiments were performed for all data. For curve Figures and bar Figures, data are presented as means ± SD. Unpaired Student's t-tests were used for comparing two variables. One-way ANOVA was used for multiple variables comparison. *, $P < 0.05$; **, $P < 0.01$; ***, $P < 0.001$; n.s., no significance in comparison with the control group.

Related to **Figure 6.**

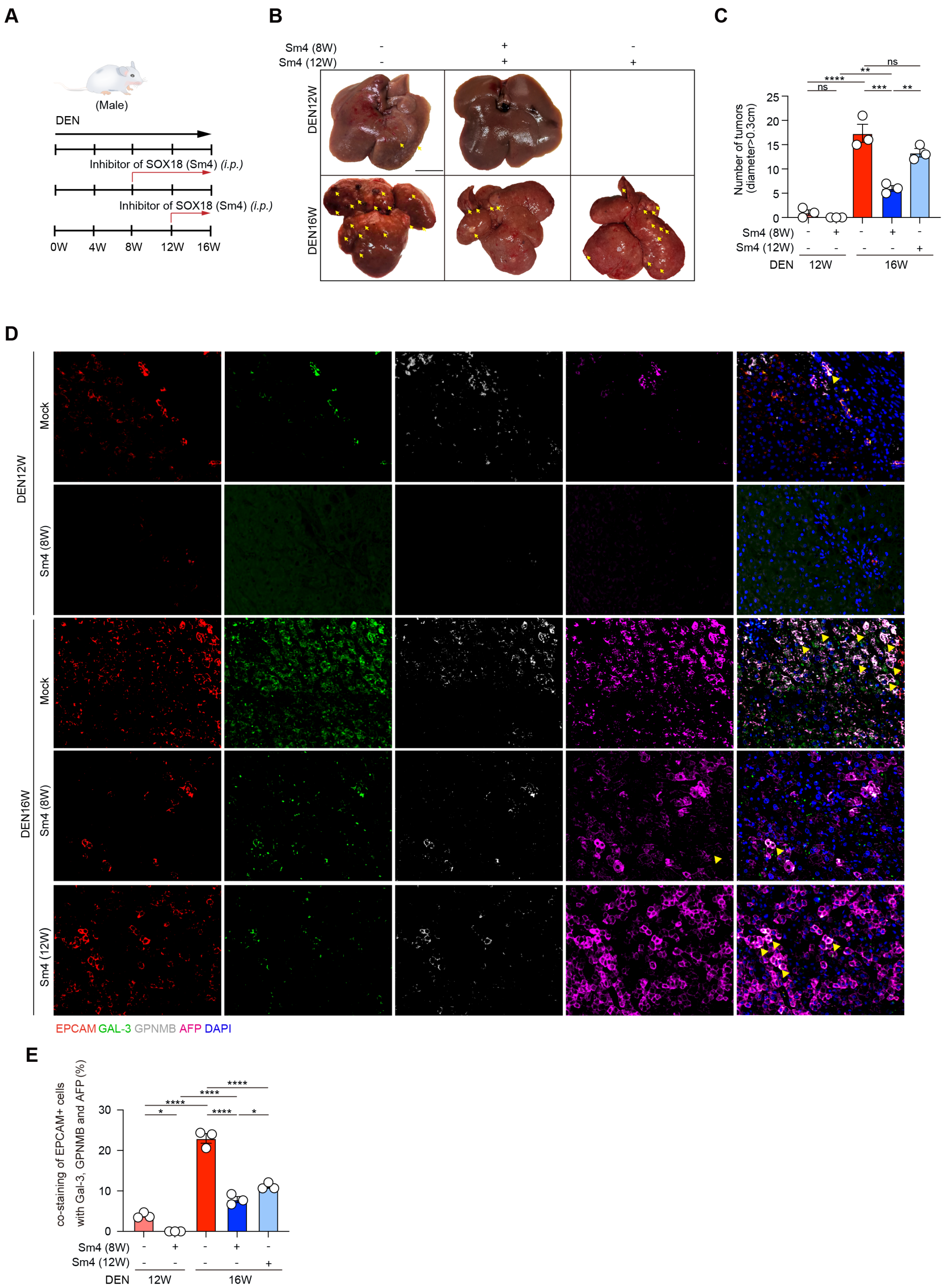

Appendix Figure S8. The role of SOX18 in the transformation of EPCAM$^+$ cells to Gal-3$^+$GPNMB$^+$ MT^{Immu} cells

A. Rats treated with inhibitor of SOX18 (Sm4) starting at 8- or 12- weeks after DEN exposure (red arrows). The rats were treated with 25 mg/kg Sm4 or an equivalent volume of 10% DMSO in PBS once a day by oral gavage. **B**. Tumor formation (yellow arrows) in the liver of rats subjected to DEN-treatment for 12- and 16- weeks. **C**. The number of tumor nodules per liver was quantified at 12- and 16- weeks. **D**. Staining of EPCAM, GPNMB, Gal-3 and DAPI in tumors of rats subjected to DEN-treatment for 12- and 16- weeks. **E**. The percent of the $EPCAM^{+}GPNMB^{+}Gal\text{-}3^{+}AFP^{+}$ cells in D. (yellow arrows). At least three independent experiments were performed for all data. For curve figures and bar figures, data were presented as means ± SEM. One-way ANOVA with multiple comparisons was used for comparing mean of each column with the mean of every other column. *, $P<0.05$; n.s., no significance in comparison with control group.

Related to **Figure 6.**

Appendix Table S1. Function of marker genes in clusters C1-C9 in Figure 1E

Gene	Protein	Function
Hnf4a	Hepatocyte nuclear factor 4-alpha	arachidonic acid binding (1)
Agxt	pyruvate biosynthetic process	metabolic process (2)
Hes6	Hairy and enhancer of split 6 (Drosophila)	transcription, DNA-templated (3); cell differentiation (4)
Apob	Apolipoprotein B-100	lipoprotein metabolic process (5); response to carbohydrate (6)
Pon1	Serum paraoxonase/arylesterase 1	cholesterol metabolic process (7); phosphatidylcholine metabolic process (8)
Cps1	Carbamoyl-phosphate synthase	hepatic amino acid catabolism (9)
Plg	Plasminogen	extracellular matrix disassembly (10); mononuclear cell migration (11)
Car2	Carbonic anhydrase 2	morphogenesis of an epithelium (12)
Gata3	GATA-binding factor 3	cell fate commitment (13); embryonic organ development (14)
Fabp7	Fatty acid-binding protein	epithelial cell proliferation (15)
Fgl1	Fibrinogen-like protein 1	glucose metabolic process (16); cholesterol metabolic process (17)
Angptl3	Angiopoietin-like 3	lipid homeostasis (18)
Cd44	CD44 antigen	cell migration (19); cell adhesion (20)
Cd24	Signal transducer CD24	innate immunity (21)
Cd47	Leukocyte surface antigen CD47	cell proliferation (22); positive regulation of T cell activation (23)
Aldh1a1	Aldehyde dehydrogenase 1A1	metabolic programming (24); oxidation-reduction process (25)
Pzp	Alpha-1-macroglobulin	suppress T-cell function (26)
Fga	Fibrinogen alpha chain	positive regulation of peptide hormone secretion (27); immune system process (28)
Slpi	Progranulin	negative regulation of viral genome replication (29)
Ifitm1	Interferon-induced transmembrane protein 1	defense response to virus (30)
Mgp	Matrix Gla protein	cell differentiation (31)
Cd274	CD274 molecule PD-1-ligand	negative regulation of CD8-positive, alpha-beta T cell activation (32)
Kdr	Vascular endothelial growth factor receptor 2	cell fate commitment (33)
Lgals3	Galectin-3	negative regulation of T cell activation (34);

		negative regulation of T cell receptor (35)
Ccl5	C-C motif chemokine 5	negative regulation of NK cells activation (36); positive regulation of monocyte chemotaxis (37)
S100a6	Protein S100-A6	ion transmembrane transport (38)
Gpnmb	Transmembrane glycoprotein NMB	osteoblast differentiation (39); cell adhesion (40); negative regulation of T cell activation (41); negative regulation of T cell proliferation (42)
Grn	Progranulin	immune escape (43)
Mmp9	Matrix metalloproteinase-9	inhibit tumor immune surveillance (44)
Cxcl2	C-X-C motif chemokine 2	cellular response to interleukin-1 (45); inflammatory response (46)
S100a9	Protein S100-A9	inflammatory response (47); immune system process (48)

Appendix Table S2. Function of Marker Genes in Clusters HC1-HC11 in Figure 2F

Gene	Protein	Function
HNF4a	Hepatocyte nuclear factor 4-alpha	arachidonic acid binding (1)
ADIRF	Adipogenesis regulatory factor	positive regulation of fat cell differentiation (49)
ITIH3	Inter-alpha-trypsin inhibitor heavy chain H3	endopeptidase inhibitor activity (50)
IGFBP2	Insulin-like growth factor-binding protein 2	Inhibits IGF-mediated growth and developmental rates (51); negative regulation of canonical Wnt signaling pathway (52)
PON1	Serum paraoxonase / arylesterase 1	cholesterol metabolic process (7); phosphatidylcholine metabolic process (8)
AGXT	Serine--pyruvate aminotransferase	metabolic process (2)
GSTA2	Glutathione S-transferase A2	epithelial cell differentiation (53)
CCL25	C-C motif chemokine 25	immune response, negative regulation of leukocyte tethering or rolling (54)
ANG	Angiogenin	angiogenesis (55); innate immune response (56)
JUN	Transcription factor Jun	leading edge cell differentiation (57); activation-induced cell death of T cells (58)
HES1	Transcription factor HES-1	cell differentiation (59, 60)
ALDH1A1	Aldehyde dehydrogenase 1A1	metabolic programming (24); oxidation-reduction process (25)
CD47	Leukocyte surface antigen CD47	cell proliferation (22); positive regulation of T cell activation (23)
S100A9	Protein S100-A9	inflammatory response (47); immune system process (48)
CXCL17	C-X-C motif chemokine 17	Recruiting MDSC and Treg (61)
GPNMB	Transmembrane glycoprotein NMB	osteoblast differentiation (39); cell adhesion (40); negative regulation of T cell activation (41); negative regulation of T cell proliferation (42)
NQO1	NAD(P)H dehydrogenase [quinone] 1	response to oxidative stress (62)
CCL20	C-C motif chemokine 20	recruit Treg cells (63); inflammatory response (64)
LGALS2	Galectin-2	T cell homeostasis (65)
SOX4	Transcription factor SOX-4	somatic stem cell population maintenance (66); Immune evasion (67)
DEFB1	Beta-defensin 1	recruit dendritic and T cell (68)

IGF2	Cation-independent mannose-6-phosphate receptor	cell differentiation (69); enhance regulatory T-cell functions (70)
PEG10	Retrotransposon-derived protein PEG10	adipocyte differentiation (71)
ENO3	Beta-enolase	glycolysis (72); muscle development (73)
DLK1	Protein delta homolog 1	differentiation of hepatic stem cells (74)
P4HA1	Prolyl 4-hydroxylase subunit alpha-1	glycolysis (75); chemoresistance (76)
PTTG1	Securin	cell growth and metastasis (77); cell cycle (78)
EGR1	Early growth response protein 1	T cell differentiation (79)
FABP5	Fatty acid-binding protein 5	lipid metabolic process (80); glucose metabolic process (81)
CENPF	Centromere protein F	mitotic-phase progression (82)
CCNB1	G2/mitotic-specific cyclin-B1	cell-cycle G2/M progression (83)
MYC	Myc proto-oncogene protein	immune suppression (84)
UBE2C	Ubiquitin-conjugating enzyme E2 C	cell growth and invasive (85); protein ubiquitination (86)
EPCAM	Epithelial cell adhesion molecule	stem cell differentiation (87)
OV6	Ov6 protein	hepatic stem cell surface markers (88)
CD44	CD44 antigen	stem cell surface markers (87)
CD24	Signal transducer CD24	biomarker for hepatic cancer stem cells (89)
ALDH1A1	Aldehyde dehydrogenase 1A1	cell differentiation (90)
CD133	Prominin-1	cell surface; cell differentiation (91)

Appendix Table S3. Immunosuppression-related L-R pairs between MTImmu and Tex/Treg in rats or humans

Ligand-receptor pairs	Reference
Grn-Tnfrsf1b	(92)
Bag6-Ncr3	(93)
Cd112-Tigit	(94)
TNFSF9-TNFRSF9	(95)
LGALS9-CD44	(96)
LGALS9-HAVCR2	(97)
PRR3-TIGHT	(98)
SPP1-CD44	(99)

REFERENCES

1. Xu Y, Zhu Y, Hu S, Xu Y, Stroup D, Pan X, et al. Hepatocyte Nuclear Factor 4α Prevents the Steatosis-to-NASH Progression by Regulating p53 and Bile Acid Signaling (in mice). Hepatology. 2021;73(6):2251-65.
2. Just PA, Charawi S, Denis RGP, Savall M, Traore M, Foretz M, et al. Lkb1 suppresses amino acid-driven gluconeogenesis in the liver. Nat Commun. 2020;11(1):6127.
3. Kim SC, Kim CK, Axe D, Cook A, Lee M, Li T, et al. All-trans-retinoic acid ameliorates hepatic steatosis in mice by a novel transcriptional cascade. Hepatology. 2014;59(5):1750-60.
4. Germain L, Noel M, Gourdeau H, Marceau N. Promotion of growth and differentiation of rat ductular oval cells in primary culture. Cancer Res. 1988;48(2):368-78.
5. Hooper AJ, van Bockxmeer FM, Burnett JR. Monogenic hypocholesterolaemic lipid disorders and apolipoprotein B metabolism. Crit Rev Clin Lab Sci. 2005;42(5-6):515-45.
6. Noakes TD, Windt J. Evidence that supports the prescription of low-carbohydrate high-fat diets: a narrative review. Br J Sports Med. 2017;51(2):133-9.
7. Khalil A, Fulop T, Berrougui H. Role of Paraoxonase1 in the Regulation of High-Density Lipoprotein Functionality and in Cardiovascular Protection. Antioxid Redox Sign. 2021;34(3):191-200.
8. Connelly PW, Draganov D, Maguire GF. Paraoxonase-1 does not reduce or modify oxidation of phospholipids by peroxynitrite. Free radical biology & medicine. 2005;38(2):164-74.
9. Winther-Sorensen M, Galsgaard KD, Santos A, Trammell SAJ, Sulek K, Kuhre RE, et al. Glucagon acutely regulates hepatic amino acid catabolism and the effect may be disturbed by steatosis. Mol Metab. 2020;42.
10. Miles LA, Baik N, Bai H, Makarenkova HP, Kiosses WB, Krajewski S, et al. The plasminogen receptor(,) Plg-R-KT,R- is essential for mammary lobuloalveolar development and lactation. J Thromb Haemost. 2018;16(5):919-32.
11. Thaler B, Baik N, Hohensinner PJ, Baumgartner J, Panzenbock A, Stojkovic S, et al. Differential expression of Plg-R-KT and its effects on migration of proinflammatory monocyte and macrophage subsets. Blood. 2019;134(6):561-7.
12. Hu J, Spencer TE. Carbonic anhydrase regulate endometrial gland development in the neonatal uterus. Biol Reprod. 2005;73(1):131-8.
13. Gaudet P, Livstone MS, Lewis SE, Thomas PD. Phylogenetic-based propagation of functional annotations within the Gene Ontology consortium. Brief Bioinform. 2011;12(5):449-62.
14. Chou J, Provot S, Werb Z. GATA3 in Development and Cancer Differentiation: Cells GATA Have It! J Cell Physiol. 2010;222(1):42-9.
15. Hermiston ML, Green RP, Gordon JI. Chimeric-transgenic mice represent a powerful tool for studying how the proliferation and differentiation programs of intestinal epithelial cell lineages are regulated. Proc Natl Acad Sci U S A. 1993;90(19):8866-70.
16. Wu HT, Ou HY, Hung HC, Su YC, Lu FH, Wu JS, et al. A novel hepatokine, HFREP1, plays a crucial role in the development of insulin resistance and type 2 diabetes. Diabetologia. 2016;59(8):1732-42.
17. Demchev V, Malana G, Vangala D, Stoll J, Desai A, Kang HW, et al. Targeted deletion of

fibrinogen like protein 1 reveals a novel role in energy substrate utilization. Plos One. 2013;8(3):e58084.

18. Kersten S. Angiopoietin-like 3 in lipoprotein metabolism. Nat Rev Endocrinol. 2017;13(12):731-9.

19. Zhu H, Mitsuhashi N, Klein A, Barsky LW, Weinberg K, Barr ML, et al. The role of the hyaluronan receptor CD44 in mesenchymal stem cell migration in the extracellular matrix. Stem Cells. 2006;24(4):928-35.

20. Ponta H, Sherman L, Herrlich PA. CD44: from adhesion molecules to signalling regulators. Nat Rev Mol Cell Biol. 2003;4(1):33-45.

21. Chen GY, Tang J, Zheng P, Liu Y. CD24 and Siglec-10 selectively repress tissue damage-induced immune responses. Science. 2009;323(5922):1722-5.

22. Hu T, Liu H, Liang Z, Wang F, Zhou C, Zheng X, et al. Tumor-intrinsic CD47 signal regulates glycolysis and promotes colorectal cancer cell growth and metastasis. Theranostics. 2020;10(9):4056-72.

23. Nath PR, Pal-Nath D, Mandal A, Cam MC, Schwartz AL, Roberts DD. Natural Killer Cell Recruitment and Activation Are Regulated by CD47 Expression in the Tumor Microenvironment. Cancer Immunol Res. 2019;7(9):1547-61.

24. Nimmakayala RK, Leon F, Rachagani S, Rauth S, Nallasamy P, Marimuthu S, et al. Metabolic programming of distinct cancer stem cells promotes metastasis of pancreatic ductal adenocarcinoma. Oncogene. 2021;40(1):215-31.

25. Calleja LF, Yoval-Sanchez B, Hernandez-Esquivel L, Gallardo-Perez JC, Sosa-Garrocho M, Marin-Hernandez A, et al. Activation of ALDH1A1 by omeprazole reduces cell oxidative stress damage. Febs J. 2021;288(13):4064-80.

26. Finch S, Shoemark A, Dicker AJ, Keir HR, Smith A, Ong S, et al. Pregnancy Zone Protein Is Associated with Airway Infection, Neutrophil Extracellular Trap Formation, and Disease Severity in Bronchiectasis. Am J Resp Crit Care. 2019;200(8):992-1001.

27. Plow EF, Edgington TS. Lymphocyte suppressive peptides from fibrinogen are derived predominantly from the A alpha chain. J Immunol. 1986;137(6):1910-5.

28. Pickering AC, Vitry P, Prystopiuk V, Garcia B, Hook M, Schoenebeck J, et al. Host-specialized fibrinogen-binding by a bacterial surface protein promotes biofilm formation and innate immune evasion. PLoS Pathog. 2019;15(6):e1007816.

29. Özdemir S, Şengez B, Arslanoğlu A. Human immunodeficiency virus type-1 Tat protein induces secretory leukocyte protease inhibitor expression in African green monkey but not human cells. Virus genes. 2020;56(2):182-93.

30. Brass AL, Huang IC, Benita Y, John SP, Krishnan MN, Feeley EM, et al. The IFITM proteins mediate cellular resistance to influenza A H1N1 virus, West Nile virus, and dengue virus. Cell. 2009;139(7):1243-54.

31. Zhang Y, Zhao L, Wang N, Li J, He F, Li X, et al. Unexpected Role of Matrix Gla Protein in Osteoclasts: Inhibiting Osteoclast Differentiation and Bone Resorption. Mol Cell Biol. 2019;39(12).

32. Wang W, Green M, Choi JE, Gijon M, Kennedy PD, Johnson JK, et al. CD8(+) T cells regulate tumour ferroptosis during cancer immunotherapy. Nature. 2019;569(7755):270-4.

33. Choi J, Jang YJ, Dabrowska C, Iich E, Evans KV, Hall H, et al. Release of Notch activity coordinated by IL-1beta signalling confers differentiation plasticity of airway progenitors via

Fosl2 during alveolar regeneration. Nat Cell Biol. 2021;23(9):953-66.
34. Demetriou M, Granovsky M, Quaggin S, Dennis JW. Negative regulation of T-cell activation and autoimmunity by Mgat5 N-glycosylation. Nature. 2001;409(6821):733-9.
35. Hsu DK, Chen HY, Liu FT. Galectin-3 regulates T-cell functions. Immunol Rev. 2009;230(1):114-27.
36. Seo W, Shimizu K, Kojo S, Okeke A, Kohwi-Shigematsu T, Fujii SI, et al. Runx-mediated regulation of CCL5 via antagonizing two enhancers influences immune cell function and anti-tumor immunity. Nat Commun. 2020;11(1):1562.
37. Ban Y, Mai J, Li X, Mitchell-Flack M, Zhang T, Zhang L, et al. Targeting Autocrine CCL5-CCR5 Axis Reprograms Immunosuppressive Myeloid Cells and Reinvigorates Antitumor Immunity. Cancer Res. 2017;77(11):2857-68.
38. Tian ZY, Wang CY, Wang T, Li YC, Wang ZY. Glial S100A6 Degrades beta-amyloid Aggregation through Targeting Competition with Zinc Ions. Aging Dis. 2019;10(4):756-69.
39. Huang YY, Bai B, Yao YC. Prospects of osteoactivin in tissue regeneration. Expert Opin Ther Tar. 2016;20(11):1357-64.
40. Palisoc P, Vaikutis L, Model E, Omara M, Khanna D, Tsou EPS, et al. Functional Characterization of Glycoprotein Nonmetastatic Melanoma Protein B in Scleroderma Fibrosis. Arthritis Rheumatol. 2021;73:1104-5.
41. Chung JS, Ramani V, Kobayashi M, Fattah F, Popat V, Zhang S, et al. DC-HIL/Gpnmb Is a Negative Regulator of Tumor Response to Immune Checkpoint Inhibitors. Clin Cancer Res. 2020;26(6):1449-59.
42. Chung JS, Bonkobara M, Tomihari M, Cruz PA, Ariizumi K. The DC-HIL/syndecan-4 pathway inhibits human allogeneic T-cell responses. Eur J Immunol. 2009;39(4):965-74.
43. Fang WL, Zhou T, Shi H, Yao ML, Zhang D, Qian HS, et al. Progranulin induces immune escape in breast cancer via up-regulating PD-L1 expression on tumor-associated macrophages (TAMs) and promoting CD8(+) T cell exclusion (vol 40, 4, 2021). J Exp Clin Canc Res. 2022;41(1).
44. Ye Y, Kuang X, Xie Z, Liang L, Zhang Z, Zhang Y, et al. Small-molecule MMP2/MMP9 inhibitor SB-3CT modulates tumor immune surveillance by regulating PD-L1. Genome Med. 2020;12(1):83.
45. Manzer R, Wang J, Nishina K, McConville G, Mason RJ. Alveolar epithelial cells secrete chemokines in response to IL-1beta and lipopolysaccharide but not to ozone. Am J Respir Cell Mol Biol. 2006;34(2):158-66.
46. Oliveira SHP, Brito VGB, Frasnelli SCT, Ribeiro BDS, Ferreira MN, Queiroz DP, et al. Aliskiren Attenuates the Inflammatory Response and Wound Healing Process in Diabetic Mice With Periodontal Disease. Front Pharmacol. 2019;10:708.
47. Imamichi T, Uchida I, Wahl SM, McCartney-Francis N. Expression and cloning of migration inhibitory factor-related protein (MRP)8 and MRP14 in arthritis-susceptible rats. Biochem Biophys Res Commun. 1993;194(2):819-25.
48. Harman JL, Loes AN, Warren GD, Heaphy MC, Lampi KJ, Harms MJ. Evolution of multifunctionality through a pleiotropic substitution in the innate immune protein S100A9. Elife. 2020;9.
49. Ni Y, Ji C, Wang B, Qiu J, Wang J, Guo X. A Novel pro-adipogenesis factor abundant in adipose tissues and over-expressed in obesity acts upstream of PPARgamma and C/EBPalpha.

J Bioenerg Biomembr. 2013;45(3):219-28.
50. Diarra-Mehrpour M, Bourguignon J, Sesboüé R, Matteï MG, Passage E, Salier JP, et al. Human plasma inter-alpha-trypsin inhibitor is encoded by four genes on three chromosomes. European journal of biochemistry. 1989;179(1):147-54.
51. Sun LH, Zhang XB, Song QQ, Liu L, Forbes E, Tian WJ, et al. IGFBP2 promotes tumor progression by inducing alternative polarization of macrophages in pancreatic ductal adenocarcinoma through the STAT3 pathway. Cancer Lett. 2021;500:132-46.
52. Sehgal P, Kumar N, Kumar VRP, Patil S, Bhattacharya A, Kumar MV, et al. Regulation of protumorigenic pathways by Insulin like growth factor binding protein2 and its association along with beta-catenin in breast cancer lymph node metastasis. Mol Cancer. 2013;12.
53. Ishikawa T, Kobayashi M, Yanagi S, Kato C, Takashima R, Kobayashi E, et al. Human Induced Hepatic Lineage-Oriented Stem Cells: Autonomous Specification of Human iPS Cells toward Hepatocyte-Like Cells without Any Exogenous Differentiation Factors. Plos One. 2015;10(4).
54. Xu BP, Deng C, Wu X, Ji T, Zhao L, Han YH, et al. CCR9 and CCL25: A review of their roles in tumor promotion. J Cell Physiol. 2020;235(12):9121-32.
55. Fagiani E, Christofori G. Angiopoietins in angiogenesis. Cancer Lett. 2013;328(1):18-26.
56. Hooper LV, Stappenbeck TS, Hong CV, Gordon JI. Angiogenins: a new class of microbicidal proteins involved in innate immunity. Nat Immunol. 2003;4(3):269-73.
57. Lammermann T, Renkawitz J, Wu XW, Hirsch K, Brakebusch C, Sixt M. Cdc42-dependent leading edge coordination is essential for interstitial dendritic cell migration. Blood. 2009;113(23):5703-10.
58. Baumann S, Hess J, Eichhorst ST, Krueger A, Angel P, Krammer PH, et al. An unexpected role for FosB in activation-induced cell death of T cells. Oncogene. 2003;22(9):1333-9.
59. Sang LY, Roberts JM, Coller HA. Hijacking HES1: how tumors co-opt the anti-differentiation strategies of quiescent cells. Trends Mol Med. 2010;16(1):17-26.
60. Kageyama R, Ohtsuka T, Tomita K. The bHLH gene Hes1 regulates differentiation of multiple cell types. Mol Cells. 2000;10(1):1-7.
61. Oka T, Sugaya M, Takahashi N, Takahashi T, Shibata S, Miyagaki T, et al. CXCL17 Attenuates Imiquimod-Induced Psoriasis-like Skin Inflammation by Recruiting Myeloid-Derived Suppressor Cells and Regulatory T Cells. J Immunol. 2017;198(10):3897-908.
62. Dimri M, Humphries A, Laknaur A, Elattar S, Lee TJ, Sharma A, et al. NAD(P)H Quinone Dehydrogenase 1 Ablation Inhibits Activation of the Phosphoinositide 3-Kinase/Akt Serine/Threonine Kinase and Mitogen-Activated Protein Kinase/Extracellular Signal-Regulated Kinase Pathways and Blocks Metabolic Adaptation in Hepatocellular Carcinoma. Hepatology. 2020;71(2):549-68.
63. Zhang CY, Qi Y, Li XN, Yang Y, Liu DL, Zhao J, et al. The role of CCL20/CCR6 axis in recruiting Treg cells to tumor sites of NSCLC patients. Biomed Pharmacother. 2015;69:242-8.
64. Affo S, Morales-Ibanez O, Rodrigo-Torres D, Altamirano J, Blaya D, Dapito DH, et al. CCL20 mediates lipopolysaccharide induced liver injury and is a potential driver of inflammation and fibrosis in alcoholic hepatitis. Gut. 2014;63(11):1782-92.
65. Sturm A, Lensch M, André S, Kaltner H, Wiedenmann B, Rosewicz S, et al. Human galectin-2: novel inducer of T cell apoptosis with distinct profile of caspase activation. J Immunol. 2004;173(6):3825-37.

66. Gracz AD, Samsa LA, Fordham MJ, Trotier DC, Zwarycz B, Lo YH, et al. Sox4 Promotes Atoh1-Independent Intestinal Secretory Differentiation Toward Tuft and Enteroendocrine Fates. Gastroenterology. 2018;155(5):1508-23 e10.
67. Bagati A, Kumar S, Jiang P, Pyrdol J, Zou AE, Godicelj A, et al. Integrin alphavbeta6-TGFbeta-SOX4 Pathway Drives Immune Evasion in Triple-Negative Breast Cancer. Cancer Cell. 2021;39(1):54-67 e9.
68. Yang D, Chertov O, Bykovskaia SN, Chen Q, Buffo MJ, Shogan J, et al. Beta-defensins: linking innate and adaptive immunity through dendritic and T cell CCR6. Science. 1999;286(5439):525-8.
69. Hedborg F, Ohlsson R, Sandstedt B, Grimelius L, Hoehner JC, Pahlman S. IGF2 expression is a marker for paraganglionic/SIF cell differentiation in neuroblastoma. Am J Pathol. 1995;146(4):833-47.
70. Yang G, Geng XR, Song JP, Wu Y, Yan H, Zhan Z, et al. Insulin-like growth factor 2 enhances regulatory T-cell functions and suppresses food allergy in an experimental model. J Allergy Clin Immunol. 2014;133(6):1702-8 e5.
71. Hishida T, Naito K, Osada S, Nishizuka M, Imagawa M. peg10, an imprinted gene, plays a crucial role in adipocyte differentiation. FEBS Lett. 2007;581(22):4272-8.
72. Moscato S, Pratesi F, Sabbatini A, Chimenti D, Scavuzzo M, Passatino R, et al. Surface expression of a glycolytic enzyme, alpha-enolase, recognized by autoantibodies in connective tissue disorders. Eur J Immunol. 2000;30(12):3575-84.
73. Keller A, Ott MO, Lamande N, Lucas M, Gros F, Buckingham M, et al. Activation of the gene encoding the glycolytic enzyme beta-enolase during early myogenesis precedes an increased expression during fetal muscle development. Mech Dev. 1992;38(1):41-54.
74. Huang J, Zhao X, Wang J, Cheng Y, Wu Q, Wang B, et al. Distinct roles of Dlk1 isoforms in bi-potential differentiation of hepatic stem cells. Stem Cell Res Ther. 2019;10(1):31.
75. Wei J, Huang K, Chen Z, Hu M, Bai Y, Lin S, et al. Characterization of Glycolysis-Associated Molecules in the Tumor Microenvironment Revealed by Pan-Cancer Tissues and Lung Cancer Single Cell Data. Cancers (Basel). 2020;12(7).
76. Xiong GF, Stewart RL, Chen J, Gao TY, Scott TL, Samayoa LM, et al. Collagen prolyl 4-hydroxylase 1 is essential for HIF-1 alpha stabilization and TNBC chemoresistance. Nat Commun. 2018;9.
77. Huang JL, Cao SW, Ou QS, Yang B, Zheng SH, Tang J, et al. The long non-coding RNA PTTG3P promotes cell growth and metastasis via up-regulating PTTG1 and activating PI3K/AKT signaling in hepatocellular carcinoma. Mol Cancer. 2018;17(1):93.
78. Quereda V, Malumbres M. Cell cycle control of pituitary development and disease. J Mol Endocrinol. 2009;42(2):75-86.
79. Yun S, Vincelette ND, Knorr KL, Almada LL, Schneider PA, Peterson KL, et al. 4EBP1/c-MYC/PUMA and NF-kappaB/EGR1/BIM pathways underlie cytotoxicity of mTOR dual inhibitors in malignant lymphoid cells. Blood. 2016;127(22):2711-22.
80. Seo J, Jeong DW, Park JW, Lee KW, Fukuda J, Chun YS. Fatty-acid-induced FABP5/HIF-1 reprograms lipid metabolism and enhances the proliferation of liver cancer cells. Commun Biol. 2020;3(1):638.
81. Hotamisligil GS, Bernlohr DA. Metabolic functions of FABPs--mechanisms and therapeutic implications. Nat Rev Endocrinol. 2015;11(10):592-605.

82. Zhu X, Mancini MA, Chang KH, Liu CY, Chen CF, Shan B, et al. Characterization of a novel 350-kilodalton nuclear phosphoprotein that is specifically involved in mitotic-phase progression. Mol Cell Biol. 1995;15(9):5017-29.
83. Wang Z, Fan M, Candas D, Zhang TQ, Qin L, Eldridge A, et al. Cyclin B1/Cdk1 coordinates mitochondrial respiration for cell-cycle G2/M progression. Dev Cell. 2014;29(2):217-32.
84. Casey SC. MYC regulates the antitumor immune response through CD47 and PD-L1 (vol 352, aaf7984, 2016). Science. 2016;353(6296):229-.
85. Jin D, Guo J, Wu Y, Du J, Wang X, An J, et al. UBE2C, Directly Targeted by miR-548e-5p, Increases the Cellular Growth and Invasive Abilities of Cancer Cells Interacting with the EMT Marker Protein Zinc Finger E-box Binding Homeobox 1/2 in NSCLC. Theranostics. 2019;9(7):2036-55.
86. Townsley FM, Aristarkhov A, Beck S, Hershko A, Ruderman JV. Dominant-negative cyclin-selective ubiquitin carrier protein E2-C/UbcH10 blocks cells in metaphase. Proc Natl Acad Sci U S A. 1997;94(6):2362-7.
87. Yovchev MI, Grozdanov PN, Joseph B, Gupta S, Dabeva MD. Novel hepatic progenitor cell surface markers in the adult rat liver. Hepatology. 2007;45(1):139-49.
88. Strain AJ, Crosby HA, Nijjar S, Kelly DA, Hubscher SG. Human liver-derived stem cells. Semin Liver Dis. 2003;23(4):373-84.
89. Yang Y, Hou J, Lin Z, Zhuo H, Chen D, Zhang X, et al. Attenuated Listeria monocytogenes as a cancer vaccine vector for the delivery of CD24, a biomarker for hepatic cancer stem cells. Cell Mol Immunol. 2014;11(2):184-96.
90. Dolle L, Best J, Empsen C, Mei J, Van Rossen E, Roelandt P, et al. Successful isolation of liver progenitor cells by aldehyde dehydrogenase activity in naive mice. Hepatology. 2012;55(2):540-52.
91. Shmelkov SV, St Clair R, Lyden D, Rafii S. AC133/CD133/Prominin-1. Int J Biochem Cell Biol. 2005;37(4):715-9.
92. Alam MS, Otsuka S, Wong N, Abbasi A, Gaida MM, Fan Y, et al. TNF plays a crucial role in inflammation by signaling via T cell TNFR2. Proc Natl Acad Sci U S A. 2021;118(50).
93. Binici J, Hartmann J, Herrmann J, Schreiber C, Beyer S, Guler G, et al. A soluble fragment of the tumor antigen BCL2-associated athanogene 6 (BAG-6) is essential and sufficient for inhibition of NKp30 receptor-dependent cytotoxicity of natural killer cells. J Biol Chem. 2013;288(48):34295-303.
94. Cheng AL, Hsu C, Chan SL, Choo SP, Kudo M. Challenges of combination therapy with immune checkpoint inhibitors for hepatocellular carcinoma. J Hepatol. 2020;72(2):307-19.
95. Daniel SK, Seo YD, Pillarisetty VG. The CXCL12-CXCR4/CXCR7 axis as a mechanism of immune resistance in gastrointestinal malignancies. Semin Cancer Biol. 2020;65:176-88.
96. Yang HL, Lai ZZ, Shi JW, Zhou WJ, Mei J, Ye JF, et al. A defective lysophosphatidic acid-autophagy axis increases miscarriage risk by restricting decidual macrophage residence. Autophagy. 2022:1-22.
97. Sharma A, Seow JJW, Dutertre CA, Pai R, Bleriot C, Mishra A, et al. Onco-fetal Reprogramming of Endothelial Cells Drives Immunosuppressive Macrophages in Hepatocellular Carcinoma. Cell. 2020;183(2):377-94 e21.
98. Solomon BL, Garrido-Laguna I. TIGIT: a novel immunotherapy target moving from bench to bedside. Cancer Immunol Immunother. 2018;67(11):1659-67.

99. Aldinucci D, Borghese C, Casagrande N. The CCL5/CCR5 Axis in Cancer Progression. Cancers (Basel). 2020;12(7).